

Understanding the Central Equatorial African long-term drought using AMIP-type simulations

Wenjian Hua^{1,2}  · Liming Zhou¹ · Haishan Chen² · Sharon E. Nicholson³ · Yan Jiang¹ · Ajay Raghavendra¹

Received: 14 November 2016 / Accepted: 28 March 2017 / Published online: 3 April 2017
© Springer-Verlag Berlin Heidelberg 2017

Abstract Previous studies show that Indo-Pacific sea surface temperature (SST) variations may help to explain the observed long-term drought during April–May–June (AMJ) since the 1990s over Central equatorial Africa (CEA). However, the underlying physical mechanisms for this drought are still not clear due to observation limitations. Here we use the AMIP-type simulations with 24 ensemble members forced by observed SSTs from the ECHAM4.5 model to explore the likely physical processes that determine the rainfall variations over CEA. We not only examine the ensemble mean (EM), but also compare the “good” and “poor” ensemble members to understand the intra-ensemble variability. In general, EM and the “good” ensemble member can simulate the drought and associated reduced vertical velocity and anomalous anti-cyclonic circulation in the lower troposphere. However, the “poor” ensemble members cannot simulate the drought and associated circulation patterns. These contrasts indicate that the drought is tightly associated with the tropical Walker circulation and atmospheric teleconnection patterns. If the observational

circulation patterns cannot be reproduced, the CEA drought will not be captured. Despite the large intra-ensemble spread, the model simulations indicate an essential role of SST forcing in causing the drought. These results suggest that the long-term drought may result from tropical Indo-Pacific SST variations associated with the enhanced and westward extended tropical Walker circulation.

Keywords Central Equatorial Africa · Drought · AMIP · Sea surface temperature

1 Introduction

The Earth’s climate has significantly changed under global warming due to increasing anthropogenic greenhouse gases (Hartmann et al. 2013). Not only are temperatures varying but rainfall variability and patterns are also changing. The impacts of climate change are not spatially uniform, and Africa is identified as one of the most vulnerable continents (Ludwig et al. 2013). Recent studies on African climate have focused mostly on the interannual to decadal variability in rainfall in West Africa, East Africa and Southern Africa (e.g., Zeng 2003; Dai et al. 2004; Hoerling et al. 2006; Giannini et al. 2008; Williams and Funk 2011; Lyon and DeWitt 2012; Maidment et al. 2015; Nicholson 2016), while Central equatorial Africa (CEA), where the second largest rainforest on the world is, has been the subject of much less investigation primarily due to the dearth of available observations (Todd and Washington 2004; Washington et al. 2013; Maidment et al. 2015). Therefore, a greater understanding of how CEA climate varies is imperative.

Few studies have attempted to understand the tropical climate system and mesoscale convective processes that determine the rainfall over CEA (e.g., Laing and Fritsch

✉ Wenjian Hua
whua@albany.edu

¹ Department of Atmospheric and Environmental Sciences, University at Albany, State University of New York, Albany, NY 12222, USA

² Key Laboratory of Meteorological Disaster, Ministry of Education (KLME)/Joint International Research Laboratory of Climate and Environment Change (ILCEC)/ Collaborative Innovation Center on Forecast and Evaluation of Meteorological Disasters (CIC-FEMD), Nanjing University of Information Science and Technology, Nanjing 210044, China

³ Earth, Ocean and Atmospheric Science, Florida State University, Tallahassee, FL 32306, USA

1993; Jackson et al. 2009; Nicholson and Grist 2003). Oceanic conditions, especially sea surface temperatures (SSTs), are the main cause of rainfall variability over Central Africa (Farnsworth et al. 2011). Camberlin et al. (2001) proposed a strong teleconnection between tropical Atlantic SSTs and CEA rainfall and a negative association of the Nino-3 SST index and rainfall in the western part of CEA (e.g., Gulf of Guinea region). Todd and Washington (2004) suggested that CEA rainfall anomalies are related to the large-scale circulation over the CEA/Atlantic region. Balas et al. (2007) examined the rainfall variability in western equatorial Africa and its links to SSTs and found that the influence of SSTs in the tropical Atlantic, Pacific and Indian Oceans is seasonally dependent.

CEA has experienced a long-term drying trend in recent decades (Malhi and Wright 2004; Asefi-Najafabady and Saatchi 2013; Diem et al. 2014). Based on multiple remote sensing data sets, Zhou et al. (2014) found a widespread decline in forest photosynthetic capacity and moisture content over the Congo Basin and attributed this large-scale decline, at least partially, to this drying trend. Hua et al. (2016) linked this drying trend to the tropical Indo-Pacific SST variations. However, the underlying physical mechanisms for this drought are still not clear due to observation limitations. Using a combined approach of observations and model simulations may provide some insight into the drying mechanisms over CEA.

General circulation models (GCMs), which are built based on physical principles and are generally able to reproduce past climate at large scales, have played a critical role in climate science and our confidence in climate simulations has been enhanced substantially in recent decades (IPCC 2013). Reliable GCMs are useful tools for understanding the physical mechanisms of climate variability and trend (Pegion and Kumar 2010) and for providing additional and supplementary information over regions with limited observations, such as CEA. Previous studies have highlighted the role of global SSTs in the cause of rainfall variability in central and eastern Africa (Todd and Washington 2004; Hoerling et al. 2006; Lyon and DeWitt 2012; Hua et al. 2016). However, fully coupled climate models still have difficulties in reproducing observed regional rainfall changes. One of the main reasons is that models cannot realistically simulate natural variations such as observed tropical SST changes (e.g., Hoerling et al. 2010). Currently the simulated rainfall changes and variability over Central Africa and other regions are still a matter of some controversy in historical simulations (e.g., Washington et al. 2013; Aloysius et al. 2016). On the other hand, Atmospheric Model Intercomparison Project (AMIP) simulations were proposed to assess the model errors and have been proven useful in addressing a number of climate change questions (Gates et al. 1999). In AMIP simulations,

SSTs and sea ice concentrations are prescribed according to observations. Given the large uncertainties in describing the connections between rainfall and SSTs from fully coupled climate models, AMIP simulations provide an effective way to examine atmospheric responses and rainfall changes to the SST perturbations.

This study aims to examine and attribute the recent long-term drying trend over CEA in the AMIP simulations from the ECHAM4.5 model. We will address the following four scientific questions: (1) Can the AMIP simulations reproduce the mean rainfall climatology over CEA? (2) Can the AMIP simulations reproduce the observed drying trend? (3) What causes the CEA drought in the AMIP simulations? (4) Are the physical mechanisms for the drought in the model consistent with the observations? Answering these questions will help to attribute the long-term drought and to improve our understanding of the physical processes that determine the CEA rainfall variability related to SST forcing. The rest of this paper is organized as follows. Section 2 describes the observations, AMIP simulations, reanalysis data and methods. The results and discussion are presented in Sect. 3. The study concludes with a brief summary in Sect. 4.

2 Data and methods

2.1 Observations, model simulations and reanalysis data

This study combines both ground observations and satellite retrievals to represent rainfall quantities and characteristics. We use two observational gridded monthly rainfall data sets from the Global Precipitation Climatology Centre (GPCC; Schneider et al. 2014) at $1^\circ \times 1^\circ$ resolution (1950–2014) and version 2.2 of the Global Precipitation Climatology Project (GPCP; Adler et al. 2003) at $2.5^\circ \times 2.5^\circ$ resolution (1979–2014). GPCC is the gauge-based data, whereas GPCP provides the combined rainfall product derived from satellites and gauge measurements (together with other major improvements in merging approaches). In addition, we have examined two other gridded gauge-only data sets from Climatic Research Unit (CRU) (Harris et al. 2014) and the National Oceanographic and Atmospheric Administration (NOAA) PRECipitation REConstruction over Land (PREC/L) (Chen et al. 2002b). However, these two data sets have a dramatic decline in the number of rain gauges over CEA (not shown), particularly during the satellite era, and thus are not included into this study.

We use the AMIP-type simulations (1950 to the present) from the International Research Institute for Climate and Society (IRI) forecast model (ECHAM4.5) forced by observed monthly evolving SSTs (<http://iridl.ideo>.

columbia.edu/SOURCES/IRI/FD/). Similar AMIP products are available from many other models but have shorter records (1979 to around 2008), which cannot depict the recent drying afterwards and thus are not used. ECHAM4.5 is an atmospheric general circulation model (AGCM) from the Max-Planck Institute for Meteorology in Hamburg with a horizontal resolution of approximately $2.8^\circ \times 2.8^\circ$ and 19 vertical levels. More detailed description of the AGCM ECHAM4.5 is given in Roeckner et al. (1996). The model has 24 ensemble members initialized with slightly different atmospheric conditions starting in or before 1950. Its AMIP simulations are run with observed SSTs derived from the OISSTv2 data, but greenhouse gasses are held constant and land use forcing is fixed. These simulations have been widely used in climate change studies (e.g., Liebmann et al. 2007; Lyon and DeWitt 2012; Yang et al. 2014).

To evaluate the model performance on simulating atmospheric circulation and related fields, we use the global atmospheric reanalysis (ERA-Interim) produced by the European Centre for Medium-Range Weather Forecast (ECMWF), which employs a 4-dimensional variational (4D-Var) data assimilation (Dee et al. 2011). The monthly geopotential height and winds at different vertical levels and sea level pressure (SLP) are used for analysis.

2.2 Methods

Our study region of Central equatorial Africa (CEA) covers the broad contiguous swath of Central Africa (10°S – 8°N , 14°E – 32°E), including the Congo Basin and surrounding areas as done in Hua et al. (2016). We focus only on the 3-month period of April, May and June (AMJ), when the drying trend is most significant and its impacts on vegetation photosynthetic capacity are most pronounced (Zhou et al. 2014; Hua et al. 2016).

To analyze the effect of SST variations on atmospheric circulation and rainfall, we use the AMIP-type simulations described above. Note that the ensemble mean (referred to as EM) is supposed to provide a more robust estimate of the forced climate signals than any individual runs and could reduce the uncertainties associated with internal variability (e.g., Deser et al. 2012). We also choose the “good” and “poor” ensemble members, which represent the best and worst simulations of the CEA drought, to examine the intra-ensemble variability and explore alternative ways of attributing the drought. The “good” and “poor” ensemble members are selected based on two criteria: (1) interannual rainfall correlations with observations during the period 1950–2014 and (2) linear rainfall trends since 1979. The “good” ones have the strongest and statistically significant correlation and the significant drying trend that can best reproduce the

observations, while the “poor” ones have the opposite. Both the ensemble mean and individual runs are included in the present study.

Two approaches are used to quantify and attribute the long-term drought over CEA. First, atmospheric circulation and related climate variables are investigated using composite analysis. As discussed by previous studies (e.g., Zhou et al. 2014; Hua et al. 2016) and shown below in our results, CEA rainfall has decreased significantly since the late 1990s. The recent period 2000–2014 and the period 1979–1993 are tagged as the dry and wet period, respectively, in line with Hua et al. (2016). The differences between these two periods are calculated in order to examine the rainfall and associated changes in atmospheric circulation. Note that these two periods can be defined differently when using the composite analysis method, such as the choice of the last and first 12 or 18 years, but similar results will be obtained. Second, linear trend analysis using least squares regression is also conducted to quantify the long-term drying. The slope of the regression is defined as the trend per decade and the statistical significance of the trend is determined by Student’s *t* test. These two methods should bolster our confidence if consistent results are obtained.

3 Results and discussion

3.1 Observed rainfall variability and trend

Figure 1 shows the areal mean anomalies of the CEA rainfall for the period 1950–2014 from GPCC. The anomalies have both positive and negative values before 1980s, with no statistically significant increasing/decreasing

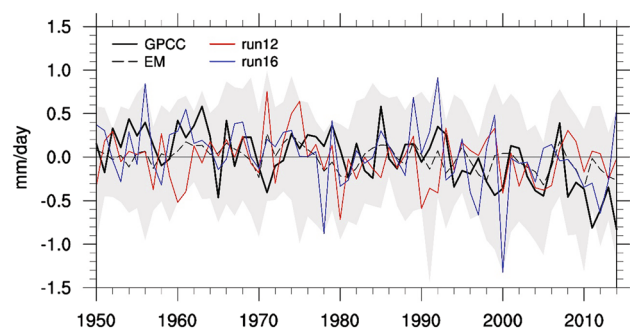


Fig. 1 The areal mean AMJ rainfall anomalies (mm/day) relative to the 1971–2000 base over Central Equatorial Africa (CEA, 10°S – 8°N , 14°E – 32°E) from GPCC (black solid line) and ensemble mean (EM, black dashed line) from the ECHAM4.5 simulations. The ECHAM4.5 ensemble ranges are indicated by shading. Red and blue solid lines indicate the individual ensemble run 12 and 16, respectively

trends. However, the rainfall has decreased significantly in the most recent decades, with a decline trend of 0.19 mm/day per decade from 1979 to 2014 ($P < 0.01$). As the data temporal coverage differs between the rainfall and reanalysis products, our focus will be on the period starting with the so-called satellite era from 1979 onward when most observations are available and the long-term drying trend is most significant over CEA.

The spatial patterns of AMJ rainfall linear trends for the period 1979–2014 are shown in Fig. 2. There is a significant decline in CEA but insignificant changes over other tropical rainforests (Amazon and South Asia). The time series of rainfall anomalies indicate a decrease in AMJ rainfall across CEA in 1998 afterwards. GPCC is in agreement with GPCP, with a correlation coefficient of 0.97 ($p < 0.01$) for the period 1979–2014 over CEA. Although GPCC and GPCP are not independent, GPCP can provide

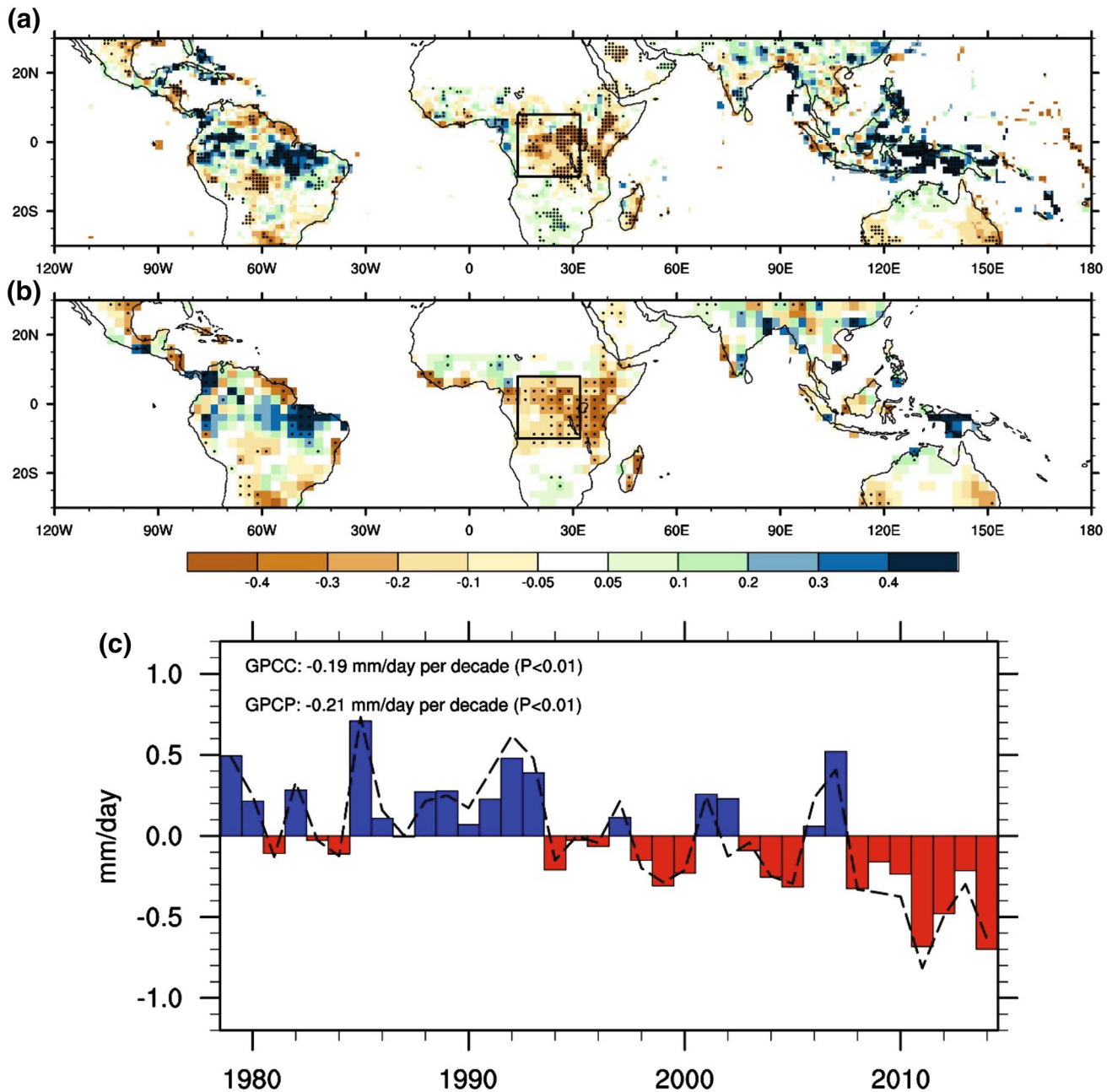


Fig. 2 Spatial patterns of AMJ rainfall linear trends (mm/day per decade) for the period 1979–2014 from **a** GPCC and **b** GPCP. The trends with *solid dots* are statistically significant at the 0.1 level.

The *rectangular box* indicates the study region of Central equatorial Africa (CEA, 10°S–8°N, 14°E–32°E). **c** The areal mean AMJ rainfall anomalies (mm/day) from GPCC (*color bar*) and GPCP (*dash line*)

more reliable information over Central Africa where there are limited in situ observations (unpublished data).

Figure 3 shows the spatial patterns of AMJ rainfall anomalies for the dry and wet periods from GPCP and GPCP, respectively. For the wet period, positive values are found over south of the Congo Basin and eastern Africa. The largest negative values basically occur in most of CEA during the dry period when there is a dramatic decrease in rainfall by more than 20% (Fig. 3b, d). The consistent spatial structures of rainfall changes between GPCP and GPCP, together with in situ observations (unpublished data) further bolster our confidence that the CEA has experienced a long-term drought and these two rainfall data sets could be used to quantify the long-term drought over CEA.

3.2 Modeled rainfall variability and trend in ensemble mean

For the ECHAM4.5 model with 24 ensemble members, we first examine whether the ensemble mean (EM) can correctly simulate the climatological features over CEA by comparing the AMJ rainfall in EM with observations (Fig. 4). The maximum in the coast of Guinea exceeding 6 mm/day observed from GPCP and GPCP is also evident in the model. The tropical rain belt located north of the equator is also reproduced by the model, although the model overestimates the amount of rainfall over the western Congo Basin and Ethiopian highlands in eastern

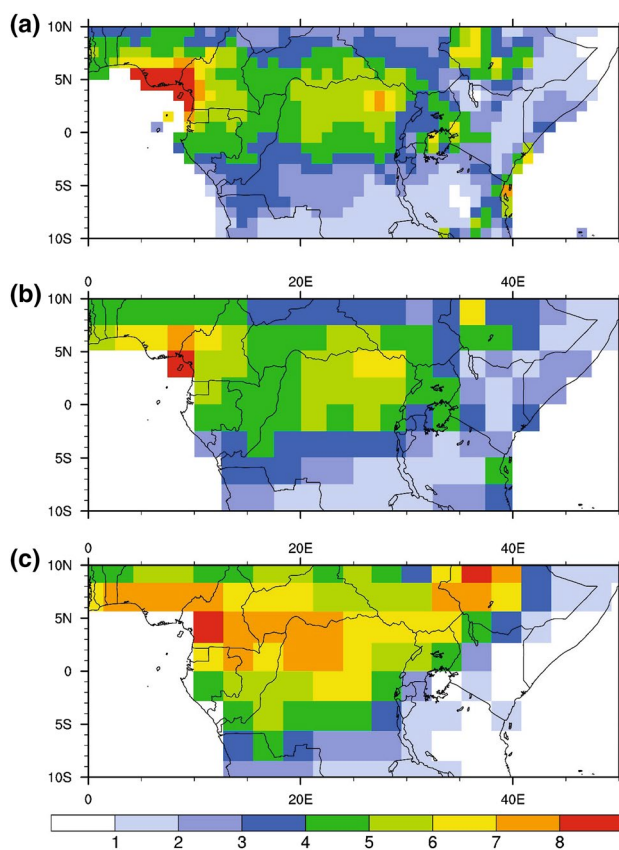


Fig. 4 Spatial patterns of climatological AMJ rainfall (mm/day) from a GPCP, b GPCP and c ECHAM4.5 ensemble mean

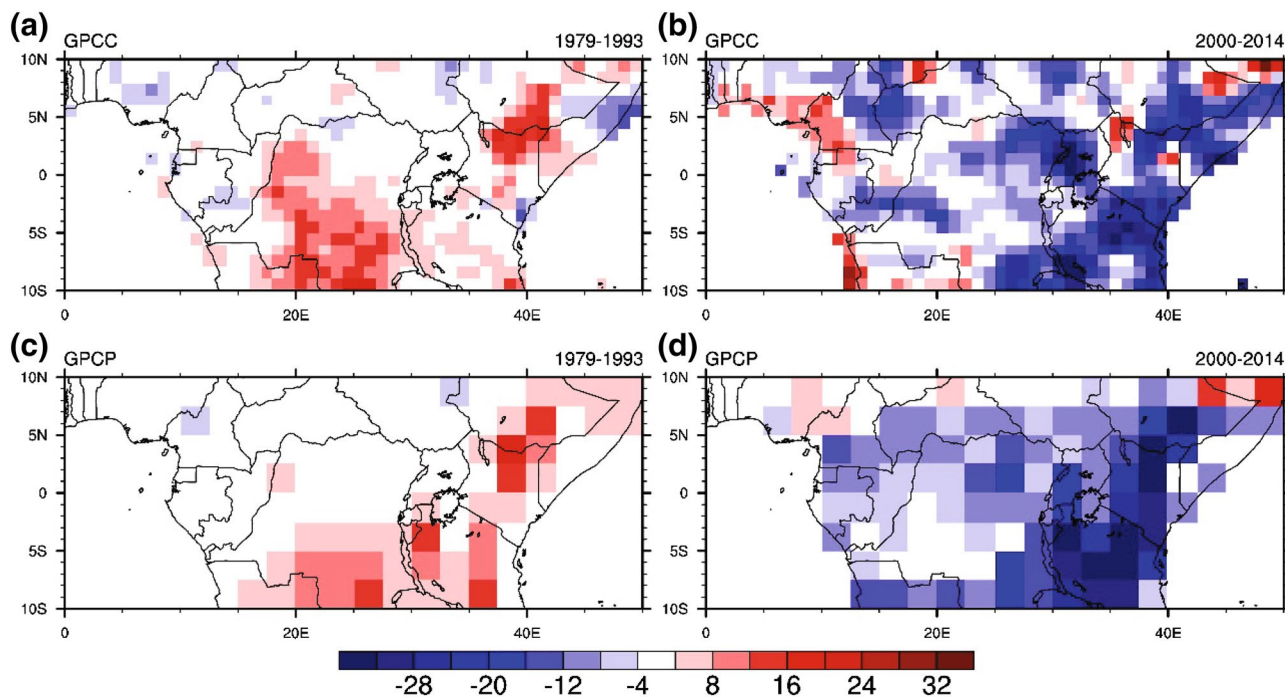


Fig. 3 Spatial patterns of AMJ rainfall percentage difference (relative to the 1979–2000 mean, unit: %) for the period a 1979–1993 and b 2000–2014 from GPCP, and c 1979–1993 and d 2000–2014 from GPCP

Africa. Overall, the latitudinal position of rainfall is similar between modeled and observed, although the magnitude in the model is overestimated.

Since the model can generally reproduce the climatological rainfall patterns, we then investigate whether the model can reasonably capture the observed rainfall variability and long-term drying trend. Basically, EM reasonably captures the interannual variability, with a temporal correlation of 0.40 across CEA for the period 1950–2014 ($p < 0.01$), although the magnitude is underestimated (Fig. 1). This is expected as EM amplifies the major SST-forced signals and smooths out the internal variability, while the observations, like one realization of the simulations, should have larger variability (e.g., Zhou et al. 2009, 2010).

Figure 5 displays the simulated AMJ rainfall trend for the period 1979–2014. Comparing with the observations (Fig. 2a, b), the model can capture the drying trend over equatorial Africa, especially in the Congo Basin, although the model has large drying biases in the Horn of Africa. The composite analysis also indicates a multi-decadal drought in recent decades (Fig. 6). Positive rainfall anomalies are

found in parts of the Congo Basin and eastern Africa during the wet period, whereas negative anomalies are seen in most of CEA areas during the dry period. The rainfall differences between the wet and dry periods in EM resemble the spatial pattern of trend shown in Fig. 5 (Fig. 7a).

Overall, the ensemble mean, which is considered primarily to be the forced climate signals, is generally consistent with the observations in simulating the rainfall variability and trend. It gives us confidence in the model's capability in attributing the long-term drying trend over CEA described next.

3.3 Drought linkage with changes in Walker circulation in ensemble mean

The above results indicate that the model can generally capture the observational rainfall variability and multi-decade drought over CEA. Because the rainfall variations are usually associated with the atmospheric circulations anomalies, we next examine whether the model can correctly simulate the atmospheric circulation variations and link the

Fig. 5 Spatial patterns of AMJ rainfall linear trend (mm/day per decade) for the period 1979–2014 from the ECHAM4.5 ensemble mean. The trends with *solid dots* are statistically significant at the 0.05 level

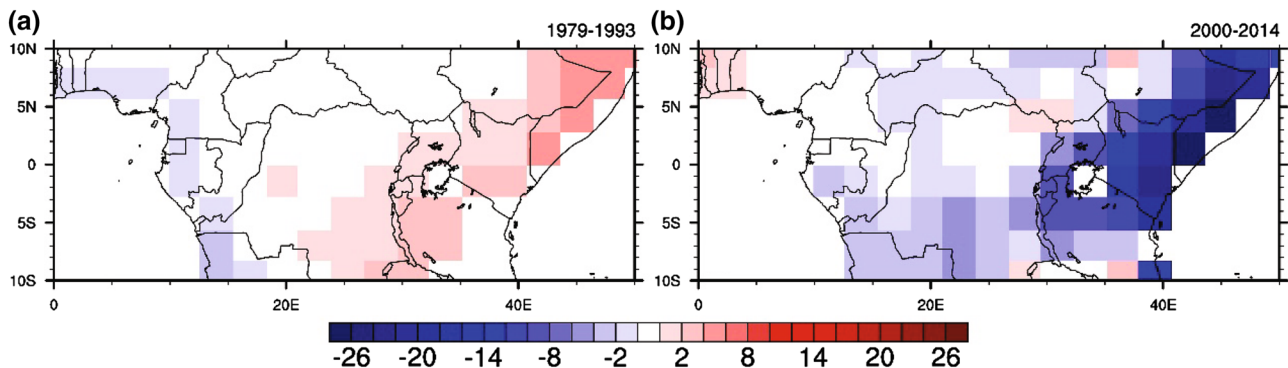
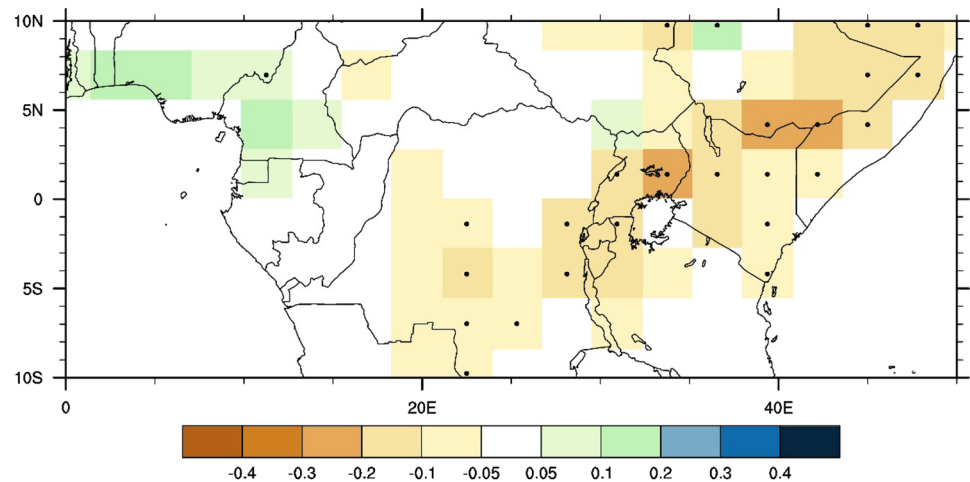


Fig. 6 Spatial patterns of AMJ rainfall percentage difference (relative to the 1979–2000 mean, unit: %) for the period **a** 1979–1993 and **b** 2000–2014 from the ECHAM4.5 ensemble mean

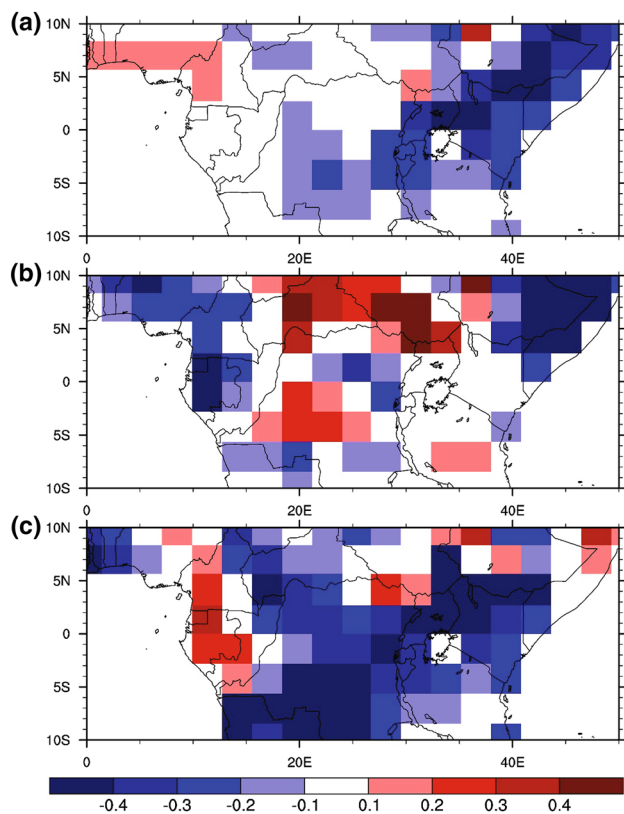


Fig. 7 The differences (2000–2014 minus 1979–1993 averages) of AMJ rainfall (mm/day) from ECHAM4.5 **a** ensemble mean, **b** run 12 and **c** run 16

drought with the changes in zonal (Walker) circulation as found in Hua et al. (2016).

EM can reproduce the prominent features of the tropical and sub-tropical circulation system in the middle and lower troposphere (Fig. 8). The AMJ mean sea level pressure (SLP) field features the subtropical highs located at roughly 30°S in the Atlantic and Indian Oceans and relatively lower pressure across the West and Central Africa continent and Arabian Peninsula. At 850 hPa, the model can also capture the winds parallel to the west coast of Africa and the southeast flow from the Indian Ocean through the coast into equatorial Africa. In addition, the model generally reproduces the Walker (zonal) circulation including upward branches over the western Pacific warm pool, eastern Indian Ocean and equatorial Africa and a downward branch over western boundary of Indian Ocean (Fig. 8c, d). On the whole, the modeled atmospheric general circulation agrees very well with the ERA-Interim reanalysis in the middle and lower troposphere (wind field and SLP), which provides the basis for examining the linkage between the atmospheric responses and rainfall changes.

What do the large-scale atmospheric circulation patterns in EM look like? Figure 9a shows the AMJ lower

troposphere winds and vertical velocity at 500 hPa. The differences between the wet and dry periods indicate that the vertical velocity weakens in association with an anomalous anti-cyclonic circulation in the lower troposphere located in western Central Africa, although the magnitude is small. It is likely that the simulated AMJ drought results, at least partially, from the large-scale atmospheric circulation changes (e.g., vertical motion and winds) induced by weaker monsoon circulation. This is consistent with the observational studies in Hua et al. (2016). On the other hand, the rainfall over Central Africa is largely influenced by the surrounding oceans and the zonal circulation due to the SSTs variations (e.g., Nicholson and Dezfuli 2013; Dezfuli et al. 2015; Cook and Vizy 2016). Funk (2012) proposed that the warming in the Indo-Pacific SSTs could enhance the export of geopotential height energy from the warm pool, which tends to induce subsidence and reduce moisture transports across eastern Africa. Hua et al. (2016) indicated the multi-decadal drought over CEA is closely linked to the changes in Walker circulation. In order to verify the impacts of zonal (Walker) circulation changes on CEA, we examine how this cell responds to the observed SST forcing. Basically, the EM can reproduce the walker circulation including the upward branches over the Indo-Pacific warm pool and Central Africa and the downward branch over the western boundary of Indian Ocean (Fig. 10a, b). Observational studies have shown that the Walker circulation has experienced a strengthening and westward shift during the late twentieth century (Chen et al. 2002a; Williams and Funk 2011; Funk 2012; Ma and Zhou 2016). When comparing the meridional mean vertical velocity during the wet period (Fig. 10a) to that of the dry period (Fig. 10b), the enhanced and westward extension of Walker circulation is clearly seen in the EM simulations (Fig. 10i).

3.4 Intra-ensemble variability

The individual ensemble members, which differ only in the initial conditions, could have a wide spread in climate responses/signals (e.g., Selten et al. 2004; Branstator and Selten 2009). For the ECHAM4.5 model, the AMIP-type simulations have deficiencies in describing the rainfall processes, which may be owing to the underlying internal atmospheric variability and their sensitivities to initial conditions (see more discussion in next section), although the ensemble runs are all forced by the same observed SSTs. For example, the ensemble results show large spread in interannual rainfall variability (shaded areas in Fig. 1), with a significant positive correlation ($r=0.39$, $p<0.01$) with observations in ensemble run 16 and a negative correlation in ensemble run 12 for the period 1950–2014. These two extreme members are selected for detailed analysis. We compare the rainfall differences between the wet and

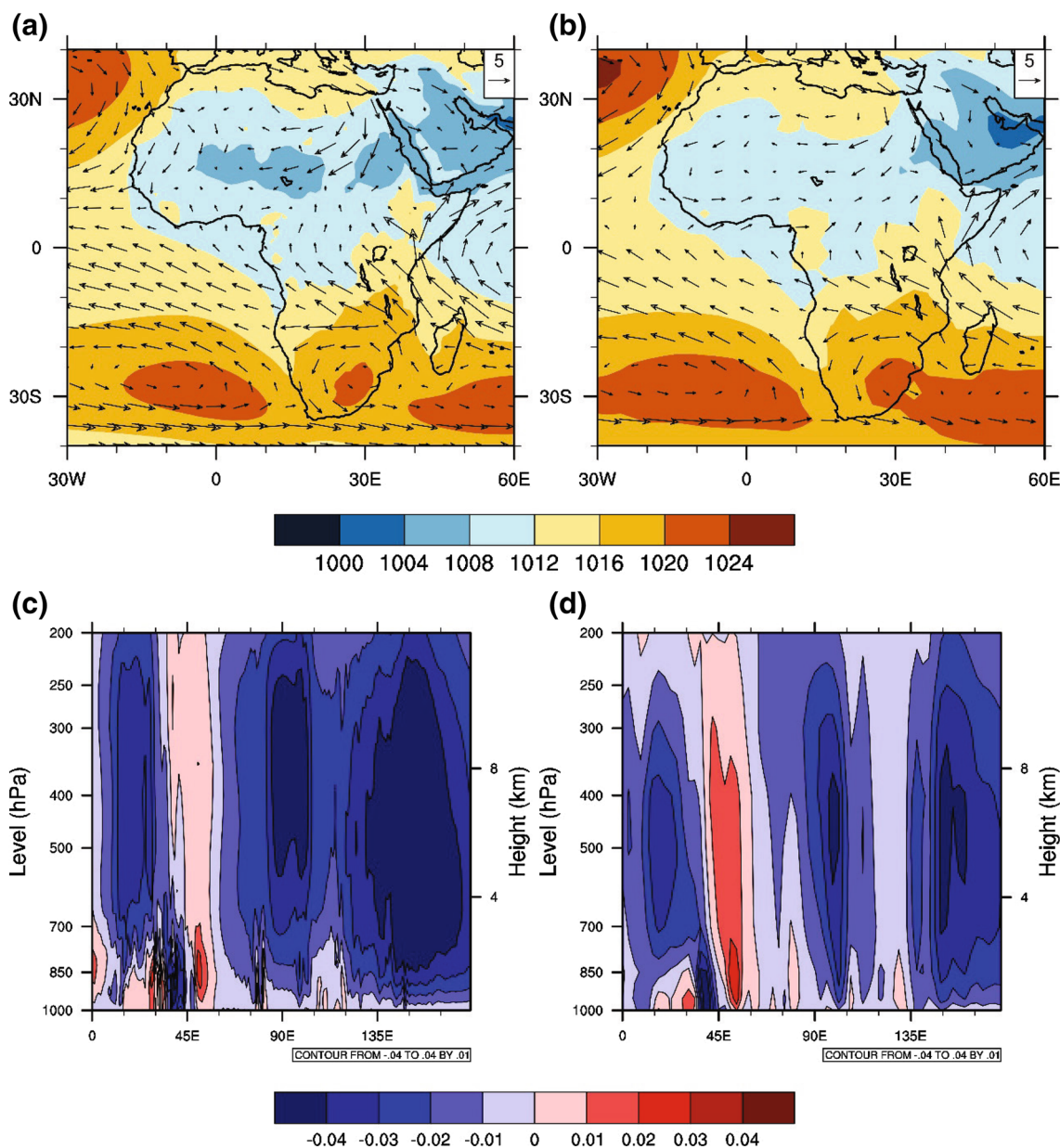


Fig. 8 Spatial patterns of climatology of AMJ sea level pressure (shading, hPa) and wind (vectors, m/s) at 850 hPa derived from **a** ERA-Interim and **b** ECHAM4.5 ensemble mean (EM) for the period

1979–2014. Spatial patterns of climatology of AMJ meridional mean (10°S–10°N) vertical velocity (ω , Pa/s) from **c** ERA-Interim and **d** ECHAM4.5 ensemble mean (EM) for the period 1979–2014

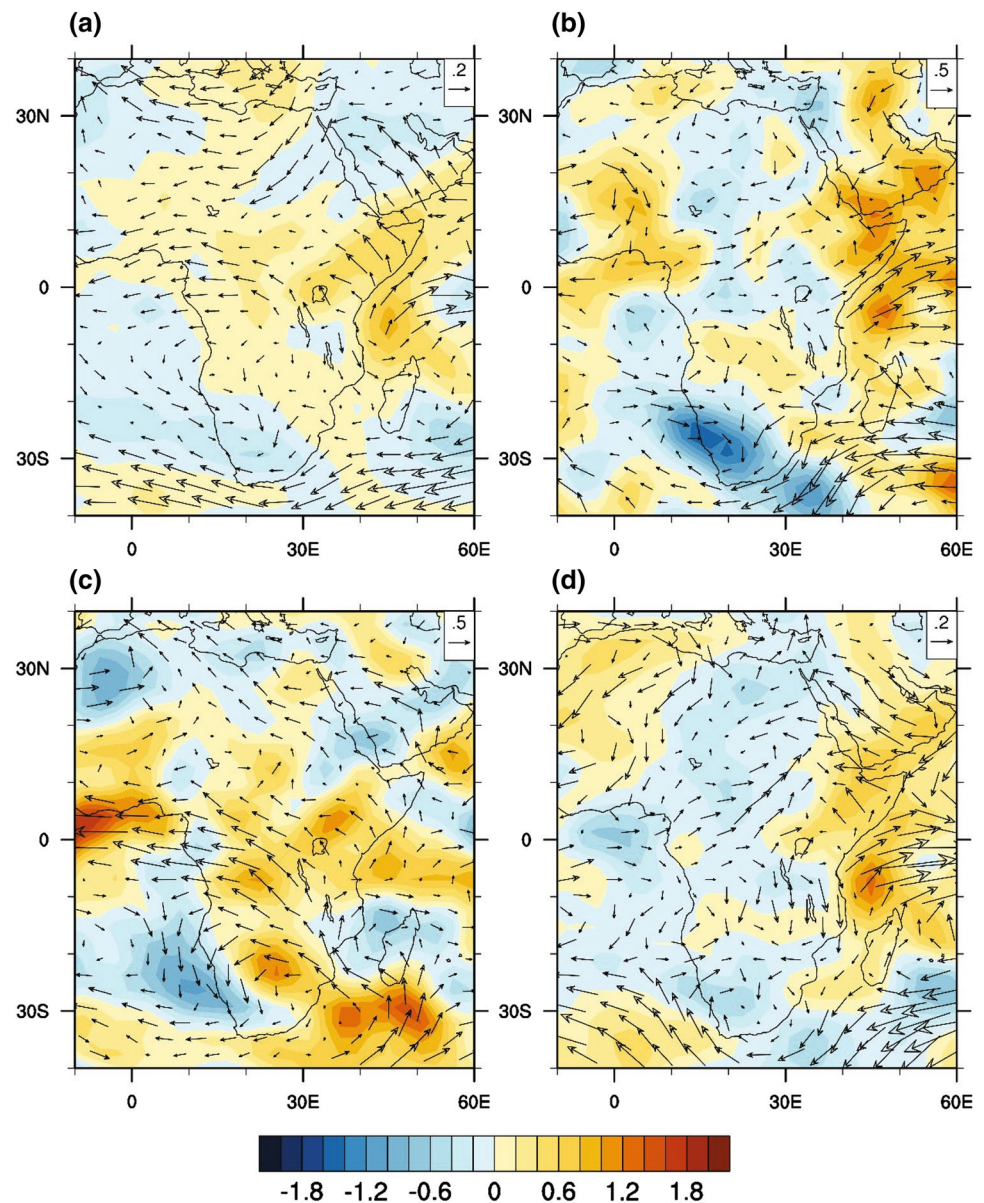
dry periods from run 12 and run 16 (Fig. 7b, c). The latter can capture the spatial patterns of rainfall decline in CEA, whereas the former cannot.

Why do the individual ensemble members from the same model with the same SSTs exhibit such a large spread? We illustrate the model behavior of climate responses by constructing the probability density function (PDF) of the regional rainfall trend. Figure 11 shows the empirical PDF of trends over CEA calculated from 24 individual members. To increase the sample size, individual trends over all grid points from the CEA region are used. On the one hand,

most of the individual members exhibit a drying trend forced by SSTs, although the amplitude and sign of trends differ among the 24 members. On the other hand, the intra-ensemble variability could be largely due to the internal atmospheric variability (e.g., Deser et al. 2012).

Next we examine the “good” and “poor” ensemble members to see how their atmospheric circulation responses differ over CEA. As shown in Fig. 9, a decrease in vertical velocity is evident over Central Africa in run 16, whereas slight ascent is found in run 12. In addition to the vertical motion, the horizontal wind fields associated with the water

Fig. 9 The differences (2000–2014 minus 1979–1993) of AMJ 850 hPa wind (vectors, m/s) and 500 hPa vertical velocity (shading, 10^2 Pa/s) from **a** ensemble mean (EM), **b** run 12, **c** run 16, and **d** the composite results in run 2, run 5, run 7 and run 12. Positive values indicate sinking motion



vapor transport modulate the rainfall variability. Run 16 features stronger southeast wind anomalies in western and central equatorial Africa than run 12 (Fig. 9b, c), suggesting reduced moisture advection from the Atlantic Ocean (e.g., Pokam et al. 2014). The subsidence associated with a reduction of low-level moisture transport toward Central Africa from the Atlantic Ocean leads to a decrease in AMJ rainfall over these areas (e.g., Hua et al. 2016). To further support our analysis, we also composite few “poor” ensemble members (run 2, run 5, run 7 and run 12). The composite results resemble these in run 12 (Fig. 9d). Our previous evaluations have shown that the “poor” ensemble members cannot reproduce the long-term drought and related circulation patterns over equatorial Africa. What are the differences in the oceanic and atmospheric teleconnection

patterns from a global perspective? In run 16, the enhanced ascent from warm pool associated with the decreased ascent over Central Africa is clearly seen, in line with the observations and the EM results (Fig. 10e, f, k). However, these features are absent in run 12 (Fig. 10c, d) and the composite results in run 2, run 5, run 7 and run 12 (Fig. 10g, h), and instead the simulated vertical velocity decreases in the recent decades (Fig. 10j, l), which is not consistent with the observations.

Analyzing the two extremes in AMIP simulations provides another way to attribute the long-term CEA drought. We found that the rainfall changes over CEA are tightly associated with the tropical Walker circulation and atmospheric teleconnection patterns due to the SSTs forcing. If the intensification and westward extension of the Walker

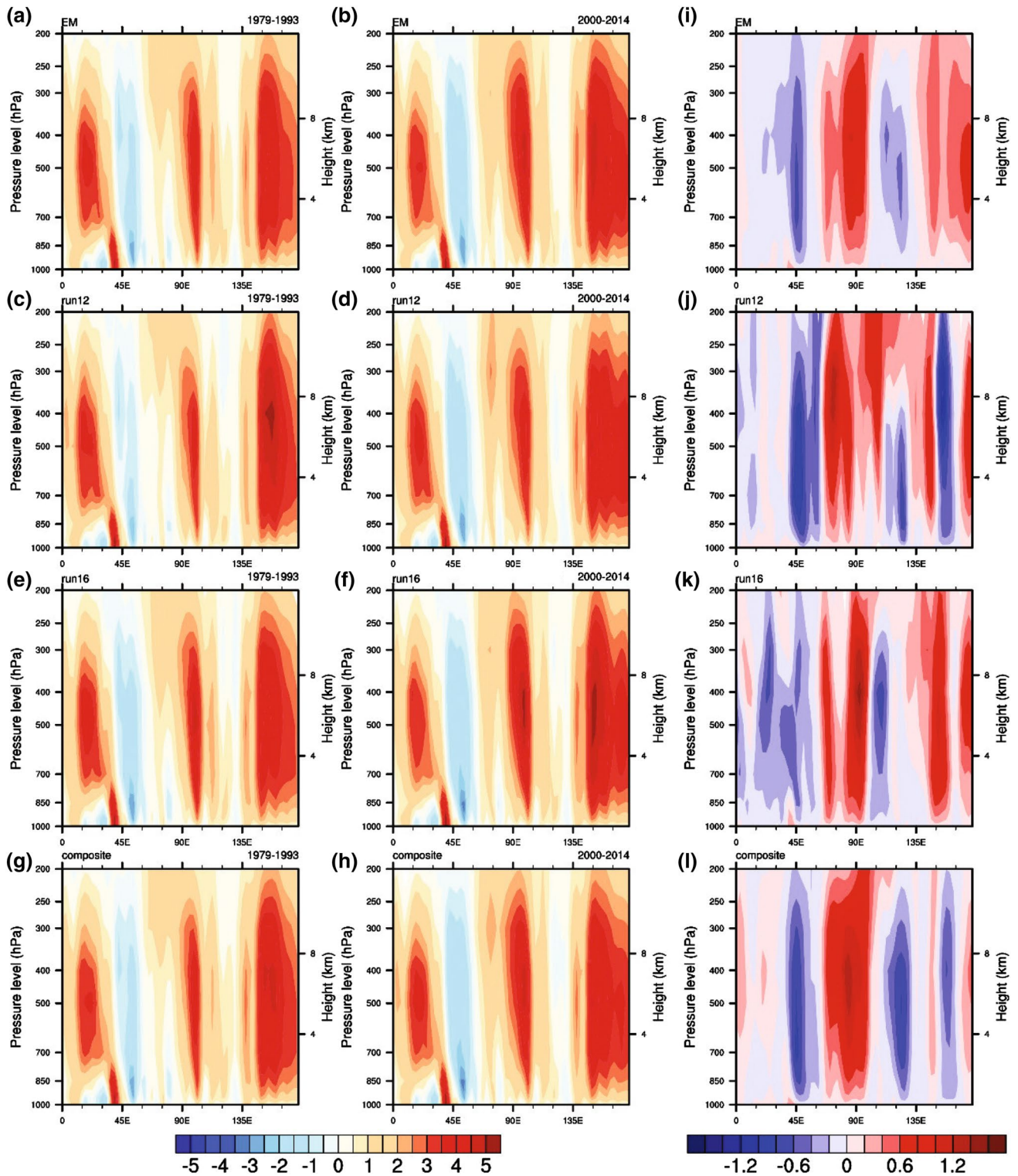


Fig. 10 **a** Climatology of AMJ meridional mean (10°S – 10°N) of vertical velocity (ω , -10^2 Pa/s) for the period 1979–1993 from ensemble mean (EM). **b** Same as **a** but for the period 2000–2014. **c** Same as **a** but from run 12. **d** Same as **b** but from run 12. **e** Same as **a** but from run 16. **f** Same as **b** but from run 16. **g** Same as **a** but from

the composite results in run 2, run 5, run 7 and run 12. **h** Same as **b** but from the composite results. **i** Differences between the wet (**a**) and dry (**b**) period. **j** Same as **i** but from run 12. **k** Same as **i** but from run 16. **l** Same as **g** but from the composite results. *Positive values indicate rising motion*

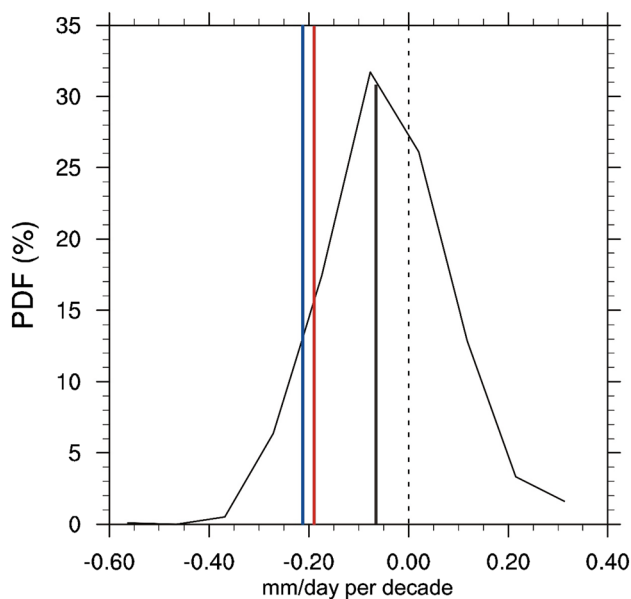


Fig. 11 The empirical probability density function (PDF) of AMJ rainfall trends during the period 1979–2014. The PDF is calculated from the 24 individual members of the AMIP simulations over all grid points over CEA. The observed trend values are indicated by the blue (GPCP) and red (GPCC) vertical line. The ensemble mean (EM) is indicated by the black vertical line

circulation cannot be reproduced in the AMIP simulations, the drying trend over CEA will not be captured. This is consistent with and provides further support to the observational findings in Hua et al. (2016).

3.5 Uncertainties in ensemble simulations

Why are the rainfall and atmospheric responses forced with the same observed SSTs different among the individual ensemble runs? Previous studies have indicated that model uncertainties mainly stem from initial conditions, boundary conditions and parameter and structural uncertainties (e.g., Tebaldi and Knutti 2007). If the model is assumed to be perfect, the uncertainties may be due to the initial and boundary conditions. For the ECHAM4.5 AMIP-type simulations, the model has 24 ensemble members initialized with slightly different atmospheric conditions but with the same observed SST forcing starting in 1950. Because the uncertainty in initial conditions increases at shorter time scales, the recent multi-decadal drought over CEA may be largely insensitive to the small variations in the initial and boundary conditions during our focused study period starting from 1979 (Tebaldi and Knutti 2007; Hawkins and Sutton 2009).

Internal atmospheric variability, also termed as climate noise or natural fluctuations of the climate system, derived from non-linear dynamical processes intrinsic to

the atmosphere, could play a dominant role in the climate changes (Deser et al. 2012). For instance, the ensemble members from the same model could exhibit a large spread in the climate change projections (e.g., Selten et al. 2004; Branstator and Selten 2009). Therefore, the intra-ensemble differences can be confounded by internal variability. To measure the uncertainty determining the CEA drought, the spread among the 24 multiple members is analyzed. The individual runs exhibit large spread based on the PDF (Fig. 11), which is probably owing to the presence of internal variability (e.g., Hoerling et al. 2006; Deser et al. 2012). Because the internal variability of the atmosphere is unpredictable, it would be helpful to perform a large number of individual runs with a “perfect” model in order to provide a robust estimate of the contribution of model’s climate signals/responses in addition to the internal variability.

Hawkins and Sutton (2009) indicated that internal variability dominates at smaller spatial scales and shorter time scales for climate change projections. In our study, we found that the internal variability may also influence the multi-decadal climate signals in the historical simulations. Hence, further work is needed to use more ensemble members to characterize the forced climate signals and uncertainties owing to the unpredictable internal variability at decadal time scales. On the other hand, the climate system is highly complex and it is fundamentally impossible to accurately describe the coupled land-ocean-atmosphere processes in one single climate model, no matter how complicated the model itself is. In addition, climate models have structural and parametric uncertainties and so may differ from the observations in both their forcing and boundary conditions (e.g., Zhou et al. 2003, 2009; Tian et al. 2004). Therefore, another way to quantify all aspects of model uncertainties is to make use of multi-model ensembles (Tebaldi and Knutti 2007; Knutti et al. 2010). The multi-model approach supplies a broader test to the models’ responses due to different physical and numerical formulations, and could provide more reliable information than a single model, which will be explored in future work. For example, the upcoming experiments simulated by multiple CMIP6-AMIP models (at least the period from 1979 to 2014) will allow us to further attribute the CEA drought and to better account for model uncertainties (Eyring et al. 2016).

The current study is focused on the role of SST forcing on the CEA drought. However, the model underestimates the magnitude of the drought, indicating that some other factors may also have some contributions. For example, changes in key land surface variables such as surface albedo, vegetation, and moisture that can influence atmospheric processes via various hydrological, biophysical, and biogeochemical mechanisms and thus potentially induce significant rainfall variability on local to regional

scales (e.g., Zhou et al. 2003, 2009; Tian et al. 2004; Hua et al. 2015; Xue et al. 2016). One major research topic on this aspect is related to land use and land cover change (LULCC) over tropical rainforests. In West Africa where deforestation and human-induced forest degradation are significant, the decreases in surface net radiation and the increases in Bowen ratio due to LULCC could result in less moisture convergence and rainfall (Wang et al. 2016; Boone et al. 2016). However, deforestation is much less significant in the Congo Basin than other tropical rainforests (Zhou et al. 2014). On the other hand, moisture recycling plays a significant role over CEA (Pokam et al. 2012) where evapotranspiration (ET) from the dense Congolese forests could contribute largely to the regional rainfall recycling. Trenberth (1999) found that the recycling activity over CEA is higher than that in the Amazon basin, suggesting the importance of land surface processes in influencing the CEA rainfall. Since Congo Basin has experienced a long-term drought and a widespread decline in forest photosynthetic capacity and moisture content, the changes in land surface properties may have modified the atmospheric exchange of carbon, water and energy, and thus have a negative feedback on the rainfall variability over the CEA. However, the land use forcing in the ECHAM4.5 simulations is fixed and so the role of land surface on the recent drought over the CEA needs to be further investigated.

4 Conclusions

Hua et al. (2016) found that the long-term drought during April-May-June (AMJ) over Central equatorial Africa (CEA) may largely result from tropical Indo-Pacific SST variations. However, the underlying physical processes for such associations are still in the exploratory stage due to observational limitations. To further this finding, we use the AMIP-type simulations with 24 ensemble members forced by observed SSTs from ECHAM4.5 model produced by International Research Institute for Climate and Society (IRI), to understand the physical processes that determine the rainfall variations over CEA. We not only examine the ensemble mean, but also choose and compare “good” and “poor” ensemble members, which represent the best and worst simulations of the CEA drought, in order to understand the intra-ensemble variability and further confirm our proposed mechanisms.

The model can generally capture the observational CEA rainfall variability and climatology, and relevant features of atmospheric circulation. The ensemble mean (EM) and the “good” ensemble member (run 16) can reproduce the multi-decadal drought over CEA, with decreasing rainfall in the Congo Basin and eastern Africa and associated reduction in vertical velocity and anomalous anti-cyclonic

circulation in the lower troposphere in western Central Africa during recent decades. They both can reproduce the observational findings (Hua et al. 2016) in terms of the zonal vertical circulation anomalies in response to observed SSTs. However, the “poor” ensemble members cannot simulate the drying and associated circulation patterns despite the same SST forcing. The contrast between the “good” and “poor” ensemble simulations give a measure of confidence that the rainfall variability over the CEA is tightly coupled with the changes in tropical Walker circulation and atmospheric teleconnection patterns. If the observational Indo-Pacific circulation cannot be reproduced, the drying trend over CEA will not be captured. These results, together with the observational analysis of Hua et al. (2016), may suggest a fundamental pattern of zonal circulation changes over tropical Indo-Pacific Ocean that determine the rainfall variations in CEA.

Despite the large intra-ensemble spread, the observational trend is located within the range of modeled trends from the 24 individual members (Fig. 11), indicating that the recent CEA drying trend may be primarily modulated by SSTs variations in the Indo-Pacific Ocean and the tropical zonal atmospheric circulation pattern. Given the uncertainties and complexities in the relationship between rainfall and atmospheric circulation associated with SSTs, more studies are needed to assess the relative roles of basin-scale SSTs driving the rainfall responses of CEA. Model approaches using idealized or specific SST-driven experiments (e.g., forced only with observed SST anomalies in Pacific Ocean) can provide a broader picture of physical mechanisms for the long-term drying over CEA.

Acknowledgements We acknowledge the International Research Institute for Climate and Society (IRI) working group on modeling, and we thank the modeling groups for producing and making their model output available. This study was supported by National Science Foundation (NSF AGS-1535426 and AGS-1535439). W.H. was jointly funded by the National Natural Science Foundation of China (41605034), the National Natural Science Foundation of Jiangsu Province (BK20160948) and the Natural Science Foundation for Higher Education Institutions in Jiangsu Province (16KJB170007) as well as project supported by the Priority Academic Program Development of Jiangsu Higher Education Institutions (PAPD). We also thank Prof. Aiguo Dai (SUNY at Albany, USA) for insightful discussion.

References

- Adler RF, Huffman GJ, Chang A, Ferraro R, Xie P, Janowiak J, Rudolf B, Schneider U, Curtis S, Bolvin D, Gruber A, Susskind J, Arkin P, Nelkin E (2003) The version-2 global precipitation climatology project (GPCP) monthly precipitation analysis (1979-present). *J Hydrometeorol* 4:1147–1167
- Aloysius NR, Sheffield J, Saiters JE, Li H, Wood EF (2016) Evaluation of historical and future simulations of precipitation and temperature in central Africa from CMIP5 climate models. *J Geophys Res* 121:130–152

- Asefi-Najafabady S, Saatchi S (2013) Response of African humid tropical forests to recent rainfall anomalies. *Phil Trans R Soc B* 368:20120306
- Balas N, Nicholson SE, Klotter D (2007) The relationship of rainfall variability in West Central Africa to sea-surface temperature fluctuations. *Int J Climatol* 27:1335–1349
- Boone AA, Xue Y, De Sales F, Comer RE, Hagos S, Mahanama S, Schiro K, Song G, Wang G, Li S, Mechoso CR (2016) The regional impact of land-use land-cover change (LULCC) over West Africa from an ensemble of global climate models under the auspices of the WAMME2 project. *Clim Dyn* 47:3547–3573
- Branstator G, Selten F (2009) Modes of variability and climate change. *J Clim* 22:2639–2658
- Camberlin P, Janicot S, Poccard I (2001) Seasonality and atmospheric dynamics of the teleconnection between African rainfall and tropical sea-surface temperature: Atlantic vs. ENSO. *Int J Climatol* 21:973–1005
- Chen J, Carlson BE, Del Genio AD (2002a) Evidence for strengthening of the tropical general circulation in the 1990s. *Science* 295:838–841
- Chen M, Xie P, Janowiak JE, Arkin PA (2002b) Global land precipitation: a 50-year monthly analysis based on gauge observations. *J Hydrometeorol* 3:249–266
- Cook KH, Vizy EK (2016) The Congo Basin Walker circulation: dynamics and connections to precipitation. *Clim Dyn* 47:697–717
- Dai A, Lamb PJ, Trenberth KE, Hulme M, Jones PD, Xie P (2004) The recent Sahel drought is real. *Int J Climatol* 24:1323–1331
- Dee DP, Uppala SM, Simmons AJ, Berrisford P, Poli P, Kobayashi S, Andrae U, Balmaseda MA, Balsamo G, Bauer P, Bechtold P, Beljaars ACM, van de Berg L, Bidlot J, Bormann N, Delsol C, Dragani R, Fuentes M, Geer AJ, Haimberger L, Healy SB, Hersbach H, Hólm EV, Isaksen L, Kållberg P, Köhler M, Matricardi M, McNally AP, Monge-Sanz BM, Morcrette J-J, Park B-K, Peubey C, de Rosnay P, Tavolato C, Thépaut J-N, Vitart F (2011) The ERA-Interim reanalysis: configuration and performance of the data assimilation system. *Quart J Roy Meteor Soc* 137:553–597
- Deser C, Phillips A, Bourdette V et al (2012) Uncertainty in climate change projections: the role of internal variability. *Clim Dyn* 38(3–4):527–546
- Dezfuli AK, Zaitchik BF, Gnanadesikan A (2015) Regional atmospheric circulation and rainfall variability in south equatorial Africa. *J Clim* 28:809–818
- Diem JE, Ryan SJ, Hartter J, Palace MW (2014) Satellite-based rainfall data reveal a recent drying trend in central equatorial Africa. *Clim Change* 126:263–272
- Eyring V, Bony S, Meehl GA, Senior CA, Stevens B, Stouffer RJ, Taylor KE (2016) Overview of the coupled model intercomparison project phase 6 (CMIP6) experimental design and organization. *Geosci Model Dev* 9:1937–1958
- Farnsworth A, White E, Williams C, Black E, Kniveton DR (2011) Understanding the large scale driving mechanisms of rainfall variability over Central Africa. In: Williams C, Kniveton D (eds) *African climate and climate change*. Springer, New York, pp 101–122
- Funk C (2012) Exceptional warming in the Western Pacific-Indian Ocean Warm Pool has contributed to more frequent droughts in Eastern Africa. *Bull Am Meteor Soc* 7:1049–1051
- Gates WL, Boyle JS, Covey C, Dease CG, Doutriaux CM, Drach RS, Fiorino M, Gleckler PJ, Hnilo JJ, Marlais SM, Phillips TJ, Potter GL, Santer BD, Sperber KR, Taylor KE, Williams DN (1999) An overview of the results of the atmospheric model intercomparison project (AMIP I). *Bull Amer Meteor Soc* 80:29–55
- Giannini A, Biasutti M, Held I M, Sobel AH (2008) A global perspective on African climate. *Clim Change* 90:359–383
- Harris I, Jones PD, Osborn TJ, Lister DH (2014) Updated high-resolution grids of monthly climatic observations—the CRU TS3.10 Dataset. *Int J Climatol* 34:623–642
- Hartmann DL, Klein Tank AMG, Rusticucci M, Alexander LV, Brönnimann S, Charabi Y, Dentener FJ, Dlugokencky EJ, Easterling DR, Kaplan A, Soden BJ, Thorne PW, Wild M, Zhai PM (2013) Observations: atmosphere and surface. In: Stocker, TF, Qin D, Plattner G-K, Tignor M, Allen SK, Boschung J, Nauels A, Xia Y, Bex V, Midgley PM (eds) *Climate change 2013: the physical science basis*. Contribution of Working Group I to the Fifth Assessment Report of the Intergovernmental Panel on Climate Change. Cambridge University Press, Cambridge, pp 159–254
- Hawkins E, Sutton R (2009) The potential to narrow uncertainty in regional climate predictions. *Bull Am Meteor Soc* 90:1095–1107
- Hoerling M, Hurrell J, Eischeid J, Phillips A (2006) Detection and attribution of twentieth-century Northern and Southern African rainfall change. *J Clim* 19:3989–4008
- Hoerling M, Eischeid J, Perlwitz J (2010) Regional precipitation trends: distinguishing natural variability from anthropogenic forcing. *J Clim* 23:2131–2145
- Hua W, Chen H, Sun S, Zhou L (2015) Assessing climatic impacts of future land use and land cover change projected with the CanESM2 model. *Int J Climatol* 35:3661–3675
- Hua W, Zhou L, Chen H, Nicholson SE, Jiang Y, Raghavendra A (2016) Possible causes of the Central Equatorial African long-term drought. *Environ Res Lett* 11:124002
- IPCC (2013) *Climate change 2013: the physical science basis*, the contribution of Working Group I to the Fifth Assessment Report of the Intergovernmental Panel on Climate Change. Cambridge University Press, Cambridge. ISBN:978-1-107-05799-1
- Jackson B, Nicholson SE, Klotter D (2009) Mesoscale convective systems over western equatorial Africa and their relationship to large-scale circulation. *Mon Wea Rev* 137:1272–1294
- Knutti R, Furrer R, Tebaldi C, Cermak J, Meehl GA (2010) Challenges in combining projections from multiple climate models. *J Clim* 23:2739–2758
- Laing A, Fritsch JM (1993) Mesoscale convective complexes in Africa. *Mon Wea Rev* 121:2254–2263
- Liebmann B, Camargo SJ, Seth A, Marengo JA, Carvalho LMV, Allured D, Fu R, Vera CS (2007) Onset and end of the rainy season in South America in observations and the ECHAM 4.5 atmospheric general circulation model. *J Clim* 20:2037–2050
- Ludwig F, Franssen W, Jans W, Beyenne T, Kruijt B, Supit I (2013) Climate change impacts on the Congo Basin region. In: Haensler A, Jacob D, Kabat P, Ludwig F (eds) *Climate change scenarios for the Congo basin*. Climate Service Centre Report No. 11, Hamburg, Germany, ISSN:2192–4058
- Lyon B, DeWitt DG (2012) A recent and abrupt decline in the East African long rains. *Geophys Res Lett* 39:L02702. doi:10.1029/2011GL050337
- Ma S, Zhou T (2016) Robust strengthening and westward shift of the tropical Pacific Walker circulation during 1979–2012: a comparison of 7 sets of reanalysis data and 26 CMIP5 models. *J Clim* 29:3097–3118
- Maidment RI, Allan RP, Black E (2015) Recent observed and simulated changes in precipitation over Africa. *Geophys Res Lett* 42:8155–8164
- Malhi Y, Wright J (2004) Spatial patterns and recent trends in the climate of tropical rainforest regions. *Phil Trans R Soc B* 359:311–329
- Nicholson SE (2016) An analysis of recent rainfall conditions in eastern Africa. *Int J Climatol* 36:526–532
- Nicholson SE, Dezfuli AK (2013) The relationship of rainfall variability in western equatorial Africa to the tropical Oceans and atmospheric circulation. Part I: The boreal spring. *J Clim* 26:45–65

- Nicholson SE, Grist JP (2003) The seasonal evolution of the atmospheric circulation over West Africa and equatorial Africa. *J Clim* 16:1013–1030
- Pegion PJ, Kumar A (2010) Multimodel estimates of atmospheric response to modes of SST variability and implications for droughts. *J Clim* 23:4327–4341
- Pokam MW, Djotang LAT, Mkankam FK (2012) Atmospheric water vapor transport and recycling in equatorial Central Africa through NCEP/NCAR reanalysis data. *Clim Dyn* 38:1715–1729
- Pokam MW, Bain CL, Chadwick RS, Graham R, Sonwa DJ, Kamba FM (2014) Identification of processes driving low-level westerlies in West Equatorial Africa. *J Clim* 27:4245–4262
- Roeckner E, Arpe K, Bengtsson L, Christoph M, Claussen M, Dümenil L, Esch M, Giorgetta M, Schlese U, Schulzweida U (1996) The atmospheric general circulation model ECHAM-4: Model description and simulation of present-day climate. Max-Planck Institute for Meteorology Tech Rep 218, Hamburg
- Schneider U, Becker A, Finger P, Meyer-Christoffer A, Ziese M, Rudolf B (2014) GPCP's new land surface precipitation climatology based on quality-controlled in situ data and its role in quantifying the global water cycle. *Theor Appl Climatol* 115:15–40
- Selten FM, Branstator GW, Dijkstra HA, Kliphuis M (2004) Tropical originals for recent and future northern hemisphere climate change. *Geophys Res Lett* 31:L21205. doi:10.1019/2004GL020739
- Tebaldi C, Knutti R (2007) The use of the multimodel ensemble in probabilistic climate projections. *Phil Trans R Soc A* 365:2053–2075
- Tian Y, Dickinson RE, Zhou L, Shaikh M (2004) Impact of new land boundary conditions from Moderate resolution imaging spectroradiometer (MODIS) data on the climatology of land surface variables. *J Geophys Res* 109:D20115. doi:10.1029/2003JD004499
- Todd MC, Washington R (2004) Climate variability in central equatorial Africa: influence from the Atlantic sector. *Geophys Res Lett* 31:L23202. doi:10.1029/2004GL020975
- Trenberth KE (1999) Atmospheric moisture recycling: role of advection and local evaporation. *J Clim* 12:1368–1381
- Wang G, Yu M, Xue Y (2016) Modeling the potential contribution of land cover changes to the late twentieth century Sahel drought using a regional climate model: impact of lateral boundary conditions. *Clim Dyn* 47:3457–3477
- Washington R, James R, Pearce H, Pokam WM, Moufouma-Okia W (2013) Congo Basin rainfall climatology: can we believe the climate models? *Phil Trans R Soc B* 368:20120296
- Williams AP, Funk C (2011) A westward extension of the warm pool leads to a westward extension of the Walker circulation, drying eastern Africa. *Clim Dyn* 37:2417–2435
- Xue Y, De Sales F, Lau WKM, Boone A, Kim KM, Mechoso CR, Wang G, Kucharski F, Schiro K, Hosaka M, Li S, Druyan LM, Sanda IS, Thiaw W, Zeng N, Comer RE, Lim YK, Mahanama S, Song G, Gu Y, Hagos SM, Chin M, Schubert S, Dirmeyer P, Leung LR, Kalnay E, Kitoh A, Lu CH, Mahowald NM, Zhang Z (2016) West African monsoon decadal variability and surface-related forcings: second West African Monsoon Modeling and Evaluation Project Experiment (WAMME II). *Clim Dyn* 47:3517–3545
- Yang W, Seager R, Cane MA, Lyon B (2014) The East African long rains in observations and models. *J Clim* 27:7185–7202
- Zeng N (2003) Drought in the Sahel. *Science* 302:999–1000
- Zhou L, Dickinson RE, Tian Y, Zeng X, Dai Y, Yang Z-Y, Schaaf CB, Gao F, Jin Y, Strahler A, Myneni RB, Yu H, Wu W, Shaikh M (2003) Comparison of seasonal and spatial variations of albedos from Moderate-Resolution Imaging Spectroradiometer (MODIS) and Common Land Mode. *J Geophys Res* 108:4488. doi:10.1029/2002JD003326
- Zhou L, Dickinson RE, Dirmeyer P, Dai A, Min S-K (2009) Spatiotemporal patterns of changes in maximum and minimum temperatures in multi-model simulations. *Geophys Res Lett* 36:L02702. doi:10.1029/2008GL036141
- Zhou L, Dickinson RE, Dai A, Dirmeyer P (2010) Detection and attribution of anthropogenic forcing to diurnal temperature range changes from 1950 to 1999: Comparing multi-model simulations with observations. *Clim Dyn* 35:1289–1307
- Zhou L, Tian Y, Myneni RB, Ciais P, Saatchi S, Liu YY, Piao S, Chen H, Vermote EF, Song C, Hwang T (2014) Widespread decline of Congo rainforest greenness in the past decade. *Nature* 509:86–90